Macromolecules
ARTICLE

Macromolecules **2009**, *42*, 9523–9527 **9523**
DOI: 10.1021/ma901239d

Structural Determination of High Density, ATRP Grown Polystyrene Brushes by Neutron Reflectivity

John R. Ell,[†] Dennis E. Mulder,[‡] Roland Faller,[‡] Timothy E. Patten,[§] and Tonya L. Kuhl*[,‡]

[†]*Department of Polymer Science and Engineering, University of Massachusetts, Amherst, Massachusetts 01003,* [‡]*Department of Chemical Engineering and Materials Science, University of California, Davis, California 95616, and* [§]*Department of Chemistry, University of California, Davis, California 95616*

Received June 9, 2009; Revised Manuscript Received October 27, 2009

ABSTRACT: The development of well-controlled synthetic schemes for growing polymer brushes directly from surfaces has recently enabled very high polymer grafting densities to be explored. Here, we report on the structure of polystyrene brushes as a function of molecular weight. The brushes were prepared by atom transfer radical polymerization (ATRP) at a high grafting density of 0.44 chains/nm^2. The dry film thickness scaled linearly with chain molecular weight. Under good solvent conditions, strongly stretched brushes of moderate molecular weight were found to maintain a parabolic density distribution consistent with theoretical predictions. Anomalous behavior was observed for higher molecular weights, suggesting that entanglements are much more pronounced in "grafted from" systems.

I. Introduction

Grafted polymer thin films and brushes are frequently formed by physisorption, chemisorption of block copolymers, or binding of end-functionalized polymer chains to surfaces.[1] These materials are a practical way to modify the mechanical or chemical properties of surfaces. Their structure, once solvated, has been studied extensively allowing an in-depth understanding of their properties and use as lubrication, adhesion, and surface compatibilization modifiers in a wide array of applications. Brush structure and hence properties depend strongly on their grafting density, σ, at the anchor surface. For example, at low grafting densities ($\sigma^* < 1$, where $\sigma^* = \sigma\pi R_g^2$ is the reduced surface density and R_g is the radius of gyration) the chains are sufficiently far apart that they can adopt coiled conformations and are in the so-called "mushroom regime". The height of the brush scales approximately as the unperturbed coil radius, $N^{3/5}$, in a good solvent. The semidilute brush regime occurs at somewhat higher grafting densities ($\sigma^* \geq 1$). These types of films have been the most studied, and the brush height scales as $N\sigma^{1/3}$. The higher exponent for N relative to the mushroom regime films indicates that the chains in semidilute brushes are stretched due to interchain repulsive interactions resulting from their closer packing. The third structural regime ($\sigma^* \gg 1$) is the "concentrated brush" or strongly stretched regime. At the extreme end of grafting levels, the equilibrium layer thickness approaches the length of a completely stretched polymer chain.[2] It is known that semidilute brush theory breaks down in the concentrated brush regime, as the scaling exponent apparently increases with increasing graft density.

Experimental studies at the very high grafting density regime are rare due to the challenges associated with forming such layers. "Grafting from" approaches provide access to this regime by polymerizing monomers directly onto a surface from solution. Typically, a monolayer of polymerization initiator is attached to a surface and polymerization occurs via monomer diffusion to the active sites of the growing polymer chains. This growth process can be contrasted to "grafting to" methods, in which the layer thickness must increase by diffusion of a polymer chain through the brush layer to the substrate surface. While several conventional and living ionic polymerization methods have been applied to the synthesis of polymer films, a recent breakthrough in the preparation of highly concentrated grafting regimes followed the development of living radical polymerization (LRP).[3−8] LRP methods have allowed for the facile preparation of grafted polymer chains with different compositions and permitted access to a large range of grafting densities using one synthetic method.[2,9−30]

Recent studies of very concentrated grafted chains have shown that their properties can differ significantly from those of semidilute brushes.[13,31] For example, poly(methyl methacrylate) brushes formed using ATRP have been found to have much better lubrication properties compared to brushes formed using "grafting to" methods, including lower friction coefficients and increased wear resistance.[32] These enhanced properties were attributed to the extremely high grafting density and covalent anchoring of the polymer layer. Fukuda and co-workers have demonstrated facile control of the grafting density, $0.07 < \sigma$ (chains/nm^2) < 0.7, and in a recent neutron surface reflectivity study, Devaux et al. reported that ultrahigh-density polystyrene (PS) brushes grafted from Si wafers using TEMPO-mediated polymerization with $\sigma = 1.1$ chains/nm^2 had very low swelling behavior in a good solvent.[13] Other affected properties include lower mechanical compressibility and higher glass transition temperatures of concentrated brushes as compared to semidilute brushes.[31]

Most literature work on using living radical polymerizations to prepare grafted polymer films has employed ellipsometry for structural characterization. Here, ATRP grown PS films were characterized using neutron reflectometry which provides higher resolution information on the film's thickness, density profile, roughness, and uniformity. Because neutrons interact with the nuclei of atoms in the film rather than electrons, radiation damage is negligible, and the contrast can be enhanced by using different isotopes (i.e., H and D) while the chemistry of the materials remains unaltered. Consequently, neutron reflectometry has

*To whom correspondence should be addressed.

Published on Web 11/13/2009

the potential to reveal significant relationships between the structure of the brushes and their methods of preparation. In this study a series of PS grafted silicon surfaces with varying molecular weights were prepared using identical reaction conditions, varying only the residence time of the substrate in the reaction vessel. Molecular weight, grafting density, thickness, and structure of the polystyrene films were characterized by neutron reflectivity as dry films and solvated brushes in the good solvent, toluene.

II. Experimental Section

Materials. All chemicals were purchased from Aldrich and Acros and used without further purification unless otherwise reported. Styrene was stirred over CaH_2 and distilled under reduced pressure to remove the inhibitor and stored at 4 °C and under N_2. Copper bromide (CuBr) was stirred in glacial acetic acid for 24 h, washed with copious amounts of ethanol, filtered, and stored under N_2 until needed. Karstedt's catalyst solution was prepared as reported by Hitchcock and Lappert.[33]

Initiator Synthesis. Allyl-11-undecane bromoisobutyrate was synthesized following established procedures.[34] In a modification to literature procedure,[34] 10-undecenyl 2-bromoisobutyrate (5.00 g, 12.2 mmol) and a stir bar were evacuated and backfilled with N_2 (3×) in an oven-dried 50 mL thick-walled Schlenk flask. Karstedt's catalyst (83 μL, 0.375 M) was added, and the flask was cooled to 0 °C.[34,35] Trichlorosilane (TCS) (4.75 mL, 47 mmol) was injected into the reaction flask under a stream of N_2. The flask was then sealed with a threaded PTFE stopper with a Viton O-ring, and the solution was allowed to warm to room temperature and later heated for 5 h at 40 °C. The solution was cooled, immediately transferred to a round-bottom flask, and vacuum-distilled at 20 mTorr at 100 °C, which yielded (3.73 g, 74%) of a clear liquid. ^{1}H NMR (600 MHz, $CDCl_3$): δ (ppm) 1.25−1.40 (16H, broad), 1.55 (2H, m), 1.65 (2H, m), 1.95 (6H, s), 4.2 (2H, t). ^{13}C NMR (150 MHz, $CDCl_3$): δ (ppm) 22, 25, 26, 28.5, 29.2, 29.3, 29.5, 29.63, 29.66, 30.9, 32.2, 55.8, 66.5, 171.4. FTIR (neat): ν (cm^{-1}) 2987, 2932, 2879, 1740.

Preparation of ATRP Grafted PS Chains. PS brushes were prepared using a modified literature procedure.[36] Single crystal silicon and quartz substrates (2 in. diameter, 1/2 in. thick) were cleaned in acetone, isopropanol, and copious amounts of water, dried, and then exposed to UV/ozone for 20 min prior to initiator self-assembly from 1 to 2 mM 11-(triethoxysilyl)-undecyl 2-bromopropionate in toluene. After drying the measured water contact angle of the initiator film was 80 ± 3°.

A custom reaction flask made to accommodate the large substrates was charged with CuBr (124 mg, 0.846 mmol), $CuBr_2$ (10 mg, 0.0432 mmol), and the initiator functionalized surface and then vacuum/backfilled three times. In a separate Schlenk flask, which was also vacuum/backfilled three times, the styrene (10 mL, 86.4 mmol), toluene (5 mL), and ethyl 2-bromoisobutyrate (13 μL, 0.09 mmol) as the sacrificial initiator were added. The solution was degassed using three freeze/pump/thaw cycles in liquid N_2. This solution was then transferred via cannula into the reaction flask followed by injection of *N,N,N′,N′,N″*-pentamethyldiethylenetriamine (PMDETA) (189 μL, 0.907 mmol) ligand. The flask was heated at 90 °C for a specified amount of time. The time to achieve a given molecular weight was estimated using calibration reactions, which used identical conditions but in the absence of a surface. Samples were taken every hour via a purged syringe to determine the molecular weights (M_n) and thereby the approximate time to terminate the brush growth for a desired molecular weight. The monomer conversion and the M_n of free chains in the supernatant were determined using GPC. The polymerization was terminated by removing the heat source, exposing the reaction to air and diluting the reaction solution with copious amounts of tetrahydrofuran (THF). The film-coated substrate was then immersed three times in fresh batches of hot toluene (200 mL) for 1 h to remove any residual polymer. The M_n and PDI of the free chains in the supernatant at the termination of the reaction were used as a measure of the grafted brush molecular weight. In all cases, the PDI was less than 1.10. Samples were stored in airtight containers until use.

Neutron Reflectivity Measurements. Specular reflectivity measured as a function of momentum transfer, $Q_z = (4\pi \sin\theta)/\lambda$, provides information on the in-plane average coherent scattering length density (SLD) profile. Neutron reflectivity measurements were performed on both the time-of-flight SPEAR reflectometer at the Manuel Lujan Neutron Scattering Center, Los Alamos National Laboratory, and the NG7 horizontal reflectometer at the Center for Neutron Research, National Institute of Standards and Technology, Gaithersburg. At SPEAR, the range of neutron wavelengths was $\lambda = 2-16$ Å with a Q_z range from 0.008 to about 0.30 $Å^{-1}$. The neutron wavelength at NG7 was 4.760 Å with a Q_z range of 0.007−0.15 $Å^{-1}$. The error bars on the data represent the statistical errors in the measurements (standard deviation, δR) where the uncertainty in the Q_z resolution, $\Delta Q_z/Q_z$, was nearly constant over this scattering vector range with a value of ~3%.

III. Results and Discussion

Dry Films. Neutron reflectivity data were collected for several substrates with different grafted PS molecular weights. The data were fit with nonlinear least-squares regression using the MOTOFIT reflectivity analysis package.[37] Figure 1 shows the reflectivity data and scattering length density (SLD) profile for dry PS films in air with M_n = 20K and 44K. The SLD model consisted of several layers: silicon substrate, 15−25 Å native oxide, 15−20 Å initiator with a SLD of 0.4×10^{-6} $Å^{-2}$, polystyrene, and air. The SLD of the polymer layer converged to 1.45×10^{-6} $Å^{-2}$ compared to the expected value of 1.42×10^{-6} $Å^{-2}$ for bulk PS, thus lending credence to the quality of the polymerization. Atomic force microscopy (AFM) showed uniform topography of the films in air with an rms roughness of 0.5 nm (5 μm × 5 μm scan size).

Figure 2 shows the dry thickness, t, of the PS layers in air versus molecular weight of the free polymer from the corresponding experiment. The PS film thickness scales linearly with molecular weight, demonstrating that the initiator layer and reaction conditions reproducibly initiate chain growth with the same grafting density and strongly suggesting that the molecular weight of the grafted chains correlates well to that found for sacrificial initiator chains growing in solution.[38] Based on a monomer repeat length of 2.6 Å,[39] the chain extension in air ranges from 25 to 31%. The grafting density was calculated by fitting the equation $t = (\sigma/\rho N_A)M_n$ to the results in Figure 2. Using a bulk PS density[40] of ρ = 1.05 g/cm^3, the average grafting density was calculated to be 0.44 chains/nm^2. The cross-sectional area of a single polystyrene chain in the crystalline state is 0.7 nm^2,[41] which yields a theoretical maximum grafting density of 1.4 chains/nm^2.

Solvated Films. For uniformly grafted polymer brushes in good solvent, both theory and simulations predict a parabolic density profile away from the surface followed by a long decaying tail.[42−46] Figure 3 shows the reflectivity data and best fit based on the SLD profile for M_n = 15K and 23K layers in deuterated toluene (SLD = 5.66×10^{-6} $Å^{-2}$). Deuterated toluene is a good solvent for polystyrene and maintains high neutron contrast to the grafted chains. After the data were acquired, the films were allowed to dry and reflectivity measurements were performed again. The profile returned to the original presolvated state, confirming that there were no changes to the film. The solvated data were analyzed using the MIRROR fitting program using

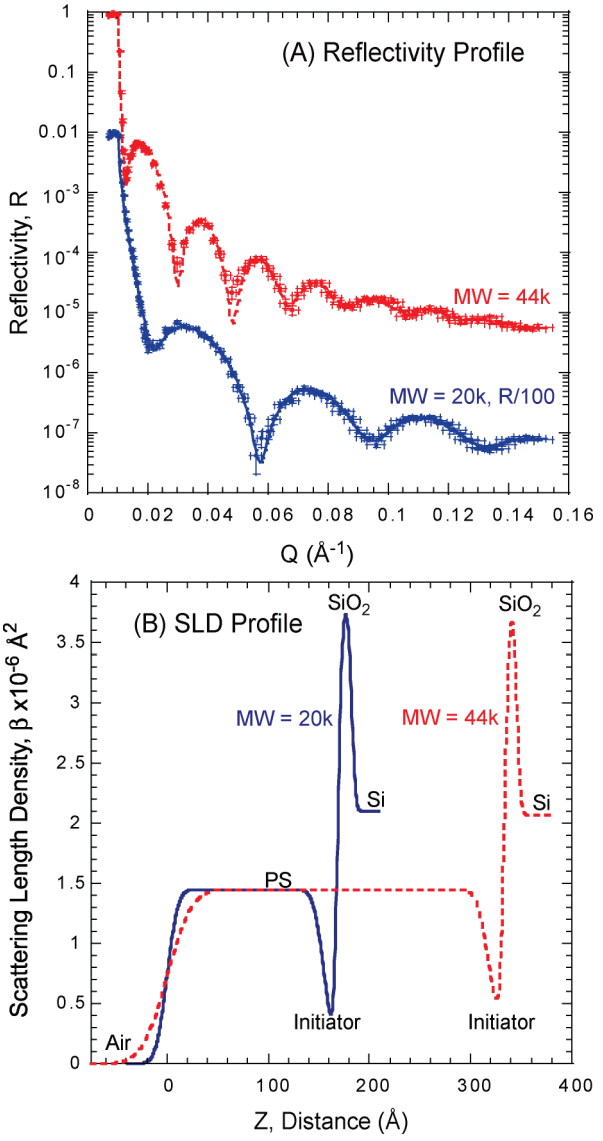

Figure 1. (A) Reflectivity profile for two different MW PS films. The 20K reflectivity profile is decreased by 2 orders of magnitude for clarity. Line fits to the data are based on the SLD profiles shown in (B).

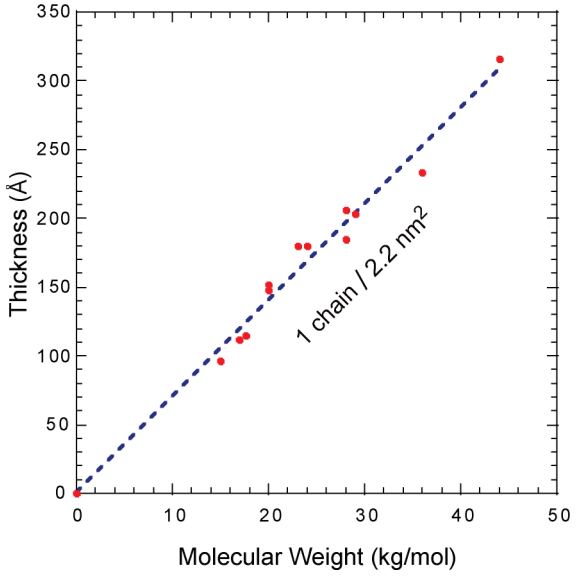

Figure 2. Thickness of dry PS films as a function of MW.

least-squares regression.[47] The region extending from the initiator was modeled with an additional layer to account for a possible depletion layer at the anchor surface followed by a power law profile for the brush with the end smeared by an error function representing the decaying tail.

To obtain the polymer brush density distribution, the SLD profile was converted to a volume fraction profile of PS extending from the initiator using $SLD_{fitted} = \phi_{PS}(SLD_{PS}) + (1 - \phi_{PS})SLD_{toluene}$. To compare with theoretical predictions, the main body of the volume fraction profiles was fitted to a power law: $\phi(z) = \phi_0(1 - (z/h_0)^n)$, where ϕ_0 is the volume fraction of the brush at the interface and h_0 is a measure of the brush extension. An important check of the physical correctness of the model fit was verified by conservation of mass where the amount of polymer in the solvated case matched to ±5% that found in the dry case. The volume fraction profiles and fitted power laws for M_n = 15K, 17K, 20K, and 23K are shown in Figure 3 and summarized in Table 1.

The profiles of the solvated brushes (Figure 3c) maintain a parabolic density profile ($n = 2.2 \pm 0.3$) away from the surface followed by a smooth exponential tail. This is in excellent agreement to previous neutron reflectivity work by Kent et al.,[48] for PS at a much lower grafting density, $\sigma <$ 0.05 chains/nm^2 and $2 < \sigma^* < 12$, compared to these ATRP grown samples, $\sigma = 0.44$ chains/nm^2 and $18 < \sigma^* < 30$. At lower grafting densities a depletion layer has been observed at the grafting surface, while at higher grafting densities small-angle neutron scattering work reveals no depletion layer with a parabolic profile and exponential tail.[49] The effect of a decreased depletion layer with increasing grafting density has also been observed in Monte Carlo simulations.[50] In the experiments here, no depletion layer was required to model the reflectivity data at these very high grafting densities.

Comparing all profiles (Figure 3c), the volume fraction at the surface increases with molecular weight. Simulations by Baranowki and Whitmore have shown the dependence of the maximum volume fraction should have a weak dependence on N and a much stronger dependence on σ scaling as $\phi_0 \propto N^{0.01}\sigma^{0.68}$.[51] The limited data range precludes a stringent testing of this dependence; however, a slightly stronger scaling with N is observed. For example, both M_n = 20K and 23K have nearly identical thicknesses and tail profiles. The increase in chain length is manifested in the increase in ϕ_0 from 0.78 to 0.85.

Although higher M_n systems were studied (Figure 2), monotonic density profiles were not obtained, suggesting that the polymerization off the substrate was less homogeneous with time or entanglements in "grafted from" systems are much more prevalent in surface polymerized brushes. To distinguish between these possibilities, we first consider the homogeneity of the reaction. In all cases, the reaction conditions for all samples were the same; only the reaction time was varied. The measured polydispersity of the supernatant free chains was also similar across all samples. There was no evidence in the GPC profile that suggested early termination or higher molecular weight coupling, e.g., tail or shoulder. The percent conversion was kept between 20% and 60% to limit termination reactions and to retain chain-end functionality.[52] Moreover, the slightly larger polydispersity obtained from solution GPC measurements for the 15K chains is consistent with the greater exponentially decaying tail shown in the SLD profile. This implies that the analysis of sacrificial chains in the supernatant is a reasonable measure of the surface grafted polymer chains, although we cannot rule out

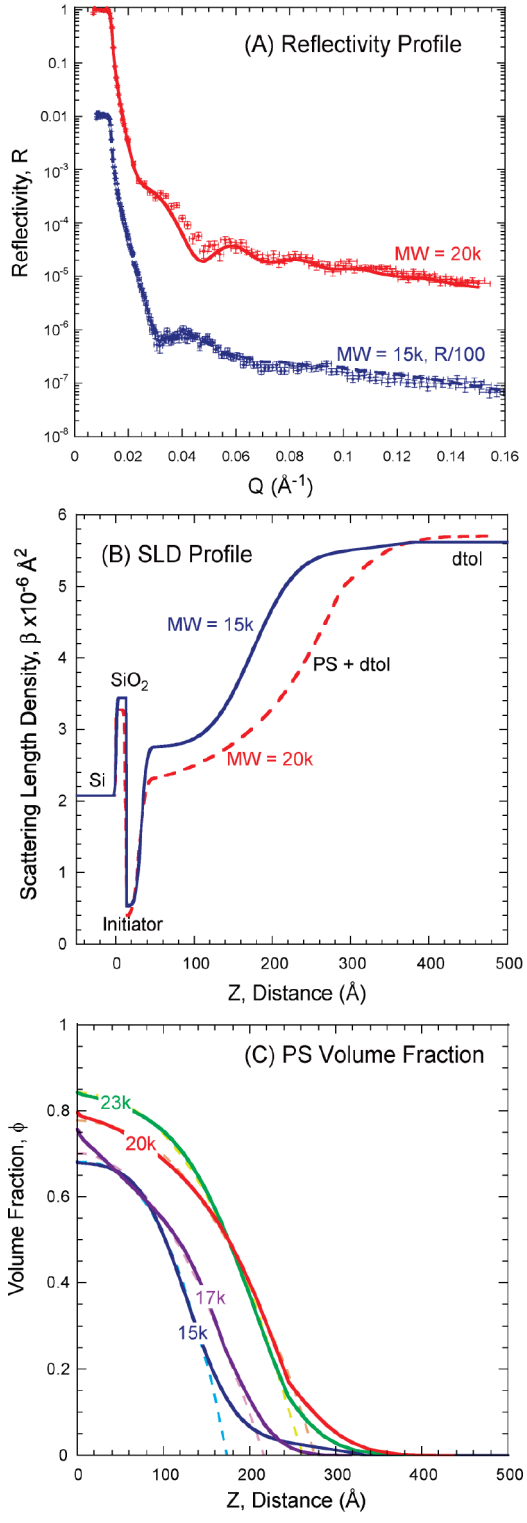

Figure 3. (A) Reflectivity profile for 15K and 20K PS in d-toluene. The 15K reflectivity profile is decreased by 2 orders of magnitude for clarity. Solid and dashed curve are fits to the data based on the SLD profiles shown in (B). (C) Volume fraction profiles of PS with power law fits (dashed).

differences between the grafted brushes and the free chains. Together, these findings suggest that variations in the polymer layer structure are not due to changes in reaction kinetics. On the other hand, the entanglement molecular weight for PS is about 18K.[53] The nonmonotonic density distributions in the higher M_n chains were consistent with small regions of higher density within the brush layer. Such

Table 1

$M_n \times 10^{-3}$ (g/mol)[a]	N	PDI[a]	h_{dry} (Å)	σ (chains/nm^2)	ϕ_0	h_0 (Å)	n
15	144	1.08	96	0.40	0.68	174	2.50
17	163	1.06	112	0.42	0.70	216	1.95
20	192	1.05	152	0.48	0.78	277	2.15
23	221	1.05	180	0.49	0.85	261	2.30

[a] Free chains in the supernatant.

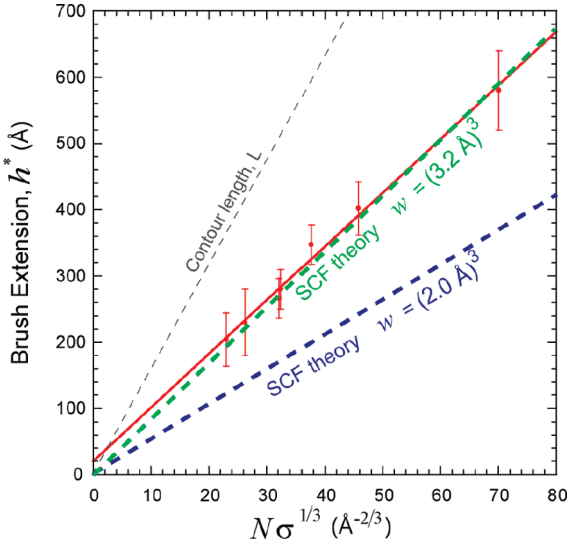

Figure 4. Estimated excluded volume parameter for polystyrene from brush extension. The extension of the brush in good solvent conditions ranges from 51% to 60% of the chain contour length.

regions could result from chain "knots" or entanglements. As the reptation time for end grafted chains to detangle is very long, the observed deviations in the density distribution profiles could result from enhanced entanglements, resulting in a lower brush extension with higher M_n systems. Taken together, these results suggest that "grafted from" systems may be more entangled due to polymerization from the substrate.

Although modeling the reflectivity data for the high-M_n brushes proved challenging, the solvated equilibrium brush height, h^*, could be estimated from the positions of the reflectivity data minima. Figure 4 shows the brush height plotted as a function of $N\sigma^{1/3}$ following the self-consistent mean-field (SCF) theory by Milner et al.[42] $h^* = (12/\pi^2)^{1/3} N\sigma^{1/3}(w/v)^{1/3}$, where w is the excluded volume parameter and $v = 3/b^2$ can be found from the statistical segment length, $b = 7.6$ Å.[54] Literature values for the excluded volume parameter for PS in toluene range from $w = (2.0$ to 2.3 Å$)^3$ via light scattering measured second virial coefficients to $w = (3.2$ Å$)^3$ from osmotic pressure experiments.[55] As shown in Figure 4, our solvated brush extensions are consistent with a larger excluded volume parameter. Such analysis offers a means to correctly estimate the molecular weight of "grafted from" chains in the absence of sacrificial chains in the reaction solution.

IV. Conclusions

Neutron reflectivity was used to study end-grafted, ATRP grown PS brushes. The synthetic procedure yielded highly reproducible polymerizations, and the grafted film thickness followed the MW obtained from sacrificial initiator in solution. In good solvent conditions, strongly stretched brushes of moderate molecular weight were found to maintain a parabolic

density distribution consistent with theoretical predictions. The relatively high grafting density gave very high volume fractions at the substrate interface ϕ_0 (0.68−0.85). Such high volume fractions should correlate with improved wear properties and potentially lower friction in tribological applications. With increasing M_n, the density distribution of the solvated brushes suggests higher density "knots" or entanglements are prevalent resulting in nonmonotonic density distributions. Further studies are needed to determine if enhanced entanglements are a general feature of "grafting from" synthesis methods.

Acknowledgment. This work was supported by the DOE under Grant ER 46340 and benefitted from the neutron research facilities of the Manual Lujan Jr. Neutron Scattering Center which is supported by DOE under Contract W7405-ENG-36 and the NIST Center for Neutron Research, DOC. This material was based on work supported by the National Science Foundation, while working at the Foundation (TEP). Any opinion, finding, and conclusions or recommendation expressed in this material are those of the author and do not necessarily reflect the views of the National Science Foundation.

References and Notes

(1) Zhao, B.; Brittain, W. J. *Prog. Polym. Sci.* **2000**, *25*, 677–710.
(2) Yamamoto, S.; Tsujii, Y.; Fukuda, T. *Macromolecules* **2000**, *33*, 5995–5998.
(3) Wang, J. S.; Matyjaszewski, K. *Macromolecules* **1995**, *28*, 7901–7910.
(4) Wang, J. S.; Matyjaszewski, K. *J. Am. Chem. Soc.* **1995**, *117*, 5614–5615.
(5) Kato, M.; Kamigaito, M.; Sawamoto, M.; Higashimura, T. *Macromolecules* **1995**, *28*, 1721–1723.
(6) Solomon, D. H.; Rizzardo, E.; Cacioli, P. 4 581 429, **1986**.
(7) Hawker, C. J. *J. Am. Chem. Soc.* **1994**, *116*, 11185–11186.
(8) Chiefari, J.; Chong, Y. K.; Ercole, F.; Krstina, J.; Jeffery, J.; Le, T. P. T.; Mayadunne, R. T. A.; Meijs, G. F.; Moad, C. L.; Moad, G.; Rizzardo, E.; Thang, S. H. *Macromolecules* **1998**, *31*, 5559–5562.
(9) Patten, T. E.; Matyjaszewski, K. *Adv. Mater.* **1998**, *10*, 1–15.
(10) Matyjaszewski, K.; Xia, J. *Chem. Rev.* **2001**, *101*, 2921–2990.
(11) Hawker, C. J. *Acc. Chem. Res.* **1997**, *30*, 373–382.
(12) Kamigaito, M.; Ando, T.; Sawamoto, M. *Chem. Rev.* **2001**, *101*, 3689–3745.
(13) Devaux, C.; Cousin, F.; Beyou, E.; Chapel, J. P. *Macromolecules* **2005**, *38*, 4296–4300.
(14) Ejaz, M.; Yamamoto, S.; Ohno, K.; Tsujii, Y.; Fukuda, T. *Macromolecules* **1998**, *31*, 5934–5936.
(15) Yamamoto, S.; Ejaz, M.; Tsujii, Y.; Fukuda, T. *Macromolecules* **2000**, *33*, 5602–5607.
(16) Samadi, A.; Husson, S. M.; Liu, Y.; Luzinov, I.; Kilbey, S. M. *Macromol. Rapid Commun.* **2005**, *26*, 1829–1834.
(17) Baum, M.; Brittain, W. J. *Macromolecules* **2002**, *35*, 610–615.
(18) de Boer, B.; Simon, H. K.; Werts, M. P. L.; van der Vegte, E. W.; Hadziioannou, G. *Macromolecules* **2000**, *33*, 349–356.
(19) Huang, W.; Kim, J.-B.; Bruening, M. L.; Baker, G. L. *Macromolecules* **2002**, *35*, 1175–1179.
(20) Huang, X.; Wirth, M. J. *Anal. Chem.* **1997**, *69*, 4577–4580.
(21) Husemann, M.; Malmstrom, E. E.; McNamara, M.; Mate, M.; Mecerreyes, D.; Benoit, D. G.; L., H. J.; Mansky, P.; Huang, E.; Russell, T. P.; Hawker, C. J. *Macromolecules* **1999**, *32*, 1424–1431.
(22) Jones, D. M.; Brown, A. A.; Huck, W. T. S. *Langmuir* **2002**, *18*, 1265–1269.
(23) Kim, J.-B.; Bruening, M. L.; Baker, G. L. *J. Am. Chem. Soc.* **2000**, *122*, 7616–7617.
(24) Kong, X.; Kawai, T.; Abe, J.; Iyoda, T. *Macromolecules* **2001**, *34*, 1837–1844.
(25) Ma, H.; Davis, R. H.; Bowman, C. N. *Macromolecules* **2000**, *33*, 331–335.
(26) Matyjaszewski, K.; Miller, P.; Shukla, N.; Immaraporn, B.; Gelman, A.; Luokala, B.; Siclovan, T.; Kickelbick, G.; Vallant, T.; Hoffmann, H.; Pakula, T. *Macromolecules* **1999**, *32*, 8716–8724.
(27) Ramakrishnan, A.; Dhamodharan, R.; Rühe, J. *Macromol. Rapid Commun.* **2002**, *23*, 612–616.
(28) Tsujii, Y.; Ejaz, M.; Sato, K.; Goto, A.; Fukuda, T. *Macromolecules* **2001**, *34*, 8872–8878.
(29) Wu, T.; Efimenko, K.; Genzer, J. *Macromolecules* **2001**, *34*, 684–686.
(30) Zhao, B.; Brittain, W. J. *J. Am. Chem. Soc.* **1999**, *121*, 3557–3558.
(31) Tsujii, Y.; Ohno, K.; Yamamoto, S.; Goto, A.; Fukuda, T. *Adv. Polym. Sci.* **2006**, *197*, 1–45.
(32) Sakata, H.; Kobayashi, M.; Otsuka, H.; Takahara, A. *Polym. J.* **2005**, *37*, 767–775.
(33) Hitchcock, P. B.; Lappert, M. F.; Warhurst, N. J. W. *Angew. Chem.* **1991**, *103*, 439−41 (see also: *Angew. Chem., Int. Ed. Engl.* **1991**, *30*, 438−40).
(34) Matyjaszewski, K.; Miller, P. J.; Shukla, N.; Immaraporn, B.; Gelman, A.; Luokala, B. B.; Siclovan, T. M.; Kickelbick, G.; Vallant, T.; Hoffmann, H.; Pakula, T. *Macromolecules* **1999**, *32*, 8716–8724.
(35) Zhao, B.; Brittain, W. J. *J. Am. Chem. Soc.* **1999**, *121*, 3557–3558.
(36) Xia, J. H.; Matyjaszewski, K. *Macromolecules* **1997**, *30*, 7697–7700.
(37) Nelson, A. *J. Appl. Crystallogr.* **2006**, *39*, 273–276.
(38) Halperin, A.; Tirrell, M.; Lodge, T. P. *Adv. Polym. Sci.* **1992**, *100*, 31–71.
(39) Sun, Q.; Faller, R. *Macromolecules* **2006**, *39*, 812–820.
(40) Mark, J. E. *Polymer Data Handbook*; Oxford University Press: New York, 1999; p xi, 1018 pp.
(41) Privalko, V. P. *Macromolecules* **1980**, *13*, 370–372.
(42) Milner, S. T.; Witten, T. A.; Cates, M. E. *Macromolecules* **1988**, *21*, 2610–2619.
(43) Factor, B. J.; Lee, L.-T.; Kent, M. S.; Rondelez, F. *Phys. Rev. E* **1993**, *48*, R2354.
(44) Murat, M.; Grest, G. S. *Macromolecules* **1989**, *22*, 4054–4059.
(45) Whitmore, M. D.; Noolandi, J. *Macromolecules* **1990**, *23*, 3321–3339.
(46) Chakrabarti, A.; Toral, R. *Macromolecules* **1990**, *23*, 2016–2021.
(47) Hamilton, W. A.; Smith, G. S.; Alcantar, N. A.; Majewski, J.; Toomey, R. G.; Kuhl, T. L. *J. Polym. Sci., Part B: Polym. Phys.* **2004**, *42*, 3290–3301.
(48) Kent, M. S.; Lee, L. T.; Factor, B. J.; Rondelez, F.; Smith, G. S. *J. Chem. Phys.* **1995**, *103*, 2320–2342.
(49) Auroy, P.; Mir, Y.; Auvray, L. *Phys. Rev. Lett.* **1992**, *69*, 93.
(50) Chen, C. M.; Fwu, Y. A. *Phys. Rev. E* **2000**, *63*, 011506.
(51) Baranowski, R.; Whitmore, M. D. *J. Chem. Phys.* **1995**, *103*, 2343–2353.
(52) Tang, W.; Matyjaszewski, K. *Macromolecules* **2007**, *40*, 1858–1863.
(53) Graessley, W. W. *The Entanglement Concept in Polymer Rheology*; Springer-Verlag: Berlin, 1974.
(54) Milner, S. T. *Europhys. Lett.* **1988**, *7*, 695–699.
(55) Ruths, M.; Johannsmann, D.; Ruhe, J.; Knoll, W. *Macromolecules* **2000**, *33*, 11.